

**IMPROVED SHAKING AND DAMAGE PARAMETERS
FOR POST-EARTHQUAKE APPLICATIONS**

Yousef Bozorgnia¹ and Vitelmo V. Bertero²

ABSTRACT

In this study, various ground shaking, response and damage parameters are examined for post-earthquake applications. Peak ground motion values, elastic response spectra, spectrum intensity, drift spectrum, inelastic spectra, and hysteretic energy spectrum are examined. Two improved damage spectra are also examined. The improved damage spectra will be zero if the response remains elastic, and will be unity when the displacement capacity under monotonic deformation is reached. Furthermore, the proposed damage spectra can be reduced to the special cases of normalized hysteretic energy and displacement ductility spectra. The proposed damage spectra are promising for various seismic vulnerability studies and post-earthquake applications.

INTRODUCTION

The objectives of this study are to examine various existing ground shaking, response and damage parameters and also to develop an improved damage parameter for post-earthquake applications. There are numerous ground shaking and damage parameters available. These include: peak ground acceleration, peak ground velocity, elastic response spectra, spectrum intensity, inelastic response spectra, interstory drift ratio, drift spectrum, hysteretic energy spectra, among others.

In this study the above parameters are examined. Additionally, improved *damage spectra* are introduced and examined in details. The damage spectra are based on normalized response quantities of a series of inelastic single-degree-of-freedom (SDOF) systems. They provide simple means for considering the demand and capacity related to strength, deformation and energy dissipation of the structural system. The proposed damage spectra will be zero if the structure remains elastic, and will be unity under the extreme condition of reaching the maximum deformation capacity under monotonically increasing lateral deformation. Following an earthquake, generation of near-real time contour maps of damage spectral ordinates can provide information on the spatial distribution of damage potential of the recorded ground motions for specified types of structures. Such maps can be useful for various post-earthquake applications, damage assessments, and emergency response; as well as for evaluation of the damage potential of earthquakes. Utilization of an up-to-date inventory of existing structures enhances the reliability of such maps in identifying the damaged areas.

Various ground shaking parameters as well as the proposed damage spectra are computed for hundreds of the ground motions recorded during the Northridge and Landers earthquakes.

¹ Principal, Applied Technology & Science (ATS), 5 Third Street, Suite 622, San Francisco, CA 94103

² Department of Civil and Environmental Engineering, University of California, Berkeley, CA 94720

Additionally, these parameters are compared for specific cases of a seven-story reinforced concrete (RC) frame, and 17 low-rise ductile RC frames affected by the Northridge earthquake.

SHAKING AND DAMAGE PARAMETERS CONSIDERED

Following an earthquake, maps of the spatial distribution of the recorded and computed data are rapidly generated and posted on the Internet by TriNet (Wald, et al., 1999). These maps are used for a wide variety of post-earthquake applications. Currently six maps are generated: contour maps of peak ground acceleration (PGA), peak ground velocity (PGV), elastic spectral accelerations at periods 0.3, 1.0, and 3.0 seconds, and instrumentally derived seismic intensity. In this study the following other ground shaking, response and damage parameters are also examined.

Damage Spectrum: Structural performance or damage limit states can be quantified by *damage indices* (DIs). A damage index is a normalized quantity that will be zero if the structure remains elastic (i.e., no significant damage is expected), and will be one if there is a potential of structural collapse. Other structural performance states (such as minor, moderate and major damages) fall in between zero and one.

Damage spectrum represents variation of a damage index versus structural period for a series of SDOF systems subjected to a recorded ground motion. Bozorgnia and Bertero (2001) introduced *two improved DIs and their corresponding damage spectra to quantify damage potential of the recorded earthquake ground motions*. The improved damage spectra explicitly satisfy the structural performance definitions at the limit states of being zero and one. Details of the definitions and characteristics of these damage spectra are presented in the following section. Damage spectra for hundreds of horizontal accelerations recorded during the Northridge and Landers earthquakes are computed, and to demonstrate an application of such spectra, contour maps of damage spectral ordinates are plotted.

Displacement Ductility: Structural damage is usually associated with inelastic response rather than elastic structural behavior. *Displacement ductility*, μ , defined as the maximum displacement of an inelastic SDOF system divided by the yield displacement, is a measure of inelastic response. Ductility spectrum, which is the variation of μ with period, can provide some useful information about general inelastic response behavior. Characteristics of inelastic spectra and the contrasts between inelastic and elastic spectra have been extensively studied for various input ground motions (e.g., Newmark and Hall, 1982; Bertero, et al., 1978; Mahin and Bertero, 1981, among other studies). Ductility spectra for hundreds of horizontal ground accelerations recorded during the Northridge and Landers, California, earthquakes are computed for 20 structural periods ranging from 0.1 to 4.0 seconds, and contours of constant ductility are presented and examined.

Interstory Drift Ratio, or more properly **Story Drift Ratio**: It is the ratio of the maximum story displacement over the story height. It has both practical and experimental significance as a measure of structural and non-structural damage. For example, for the purpose of *performance-based seismic design*, "SEAOC Blue Book" (SEAOC, 1999) has provided tentative values for drift ratios associated with different structural performance states. The interstory drift ratios demanded by the recorded ground motions are estimated using the calculated displacement ductility ratio.

Hysteretic Energy: E_H , is a measure of the inelastic energy dissipation demanded by the earthquake ground motion (Mahin and Bertero, 1981; Uang and Bertero, 1990; Bertero and Uang, 1992). Hysteretic energy includes cumulative effects of repeated cycles of inelastic response and, therefore, the effects of strong-motion duration are included in this quantity. If the response of the structure remains elastic, E_H will be zero. “Equivalent hysteretic energy velocity,” $V_H = (2 E_H/M)^{1/2}$ has also been used (Uang and Bertero, 1988), where M is the mass of the SDOF system. V_H spectra demanded by horizontal ground motions recorded in the Northridge and Landers earthquakes are also computed for a series of inelastic SDOF systems. Contours of constant V_H spectral ordinates are also plotted.

Housner Spectrum Intensity: Housner (1952) defined spectrum intensity (SI) as the area under the pseudo-velocity response spectrum over a period range of 0.1 to 2.5 seconds. It is a measure of the intensity of ground shaking for elastic structures (Housner, 1975). SI is computed for 5% damping for hundreds of horizontal ground acceleration records. Contour map of SI for the Northridge earthquake is also presented.

Drift Spectrum: This quantity represents maximum story drift ratio in multi-story buildings demanded by the ground motion (Iwan, 1997). The formulation is based on linear elastic response of a uniform continuous shear-beam model. It requires ground velocity and displacement histories as input motions. Drift spectra of the ground motions recorded during the Northridge earthquake are computed and contours of constant drift spectral ordinates are plotted.

There are other shaking parameters whose characteristics and effects directly or indirectly are included in the above parameters. For example, a parameter of interest is the duration of strong ground motion (Bolt, 1973; Trifunac and Brady, 1975). The effects of the strong-motion duration through repeated cycles of inelastic response are included in the hysteretic energy and damage spectra.

Another parameter of interest is Arias Intensity (Arias, 1970), which, in its commonly used version, is the area under the total energy spectrum in an undamped elastic SDOF system. Energy in SDOF systems is included in both V_H and damage spectra, and these parameters are evaluated over a wide range of natural periods.

In the following sections, descriptions of damage spectra and their characteristics are presented, followed by the results for the other shaking and response parameters.

DAMAGE SPECTRUM

In the following sections a brief overview of various damage indices are provided. Improved damage indices are then introduced and damage spectra are presented.

Review of Most Commonly Used Damage Indices

A damage index (DI) is based on a set of structural response parameters such as force, deformation and energy dissipation. One method of computing the DI is to compare the response parameters demanded by the earthquake with the structural “capacities” (Powell and Allahabadi, 1988). Traditionally, the “capacities” or ultimate values of the response parameters are defined in terms of their maximum values under monotonically increasing deformations. For example, a fraction of the ultimate deformation capacity of the system under monotonically increasing

lateral deformation (u_{mon}) has been used as the deformation capacity during the earthquake motion.

There are different damage indices available. For example, damage index may be based on plastic deformation (e.g., Powell and Allahabadi, 1988; Cosenza, et al., 1993):

$$DI_{\mu} = (u_{max} - u_y) / (u_{mon} - u_y) = (\mu - 1) / (\mu_{mon} - 1) \quad (1)$$

where u_{max} and u_y are the maximum and yield deformations, respectively, and u_{mon} is maximum deformation capacity of the system under a monotonically increasing lateral deformation. In equation (1) $\mu = u_{max}/u_y$ is displacement ductility demanded by the earthquake and $\mu_{mon} = u_{mon}/u_y$ is “monotonic ductility capacity”.

Displacement ductility alone does not reveal information on the repeated cycles of inelastic deformations and energy dissipation demand (e.g., Mahin and Bertero, 1981; Mahin and Lin, 1983). Hence, other structural response parameters such as hysteretic energy dissipation has also been used. Seismic input energy to a structural system (E_I) is balanced by (Uang and Bertero, 1988; and 1990):

$$E_I = E_H + E_K + E_S + E_{\xi} \quad (2)$$

where E_H , E_K , E_S and E_{ξ} are irrecoverable hysteretic energy, kinetic energy, recoverable elastic strain energy, and viscous damping energy, respectively. Hysteretic energy (E_H) includes cumulative effects of repeated cycles of inelastic response and is usually associated with the structural damage. If the response of the structure remains elastic, E_H will be zero, by its definition. For SDOF systems, Mahin and Bertero (1976; and 1981) defined normalized hysteretic energy $E_H/(F_y u_y)$ and its corresponding normalized hysteretic energy ductility:

$$\mu_H = E_H/(F_y u_y) + 1 \quad (3)$$

where F_y and u_y are yield strength and deformation of the system, respectively. Numerically μ_H is equal to the displacement ductility of a monotonically deformed equivalent elastic-perfectly-plastic (EPP) system that dissipates the same hysteretic energy, and has the same yield strength and initial stiffness as the actual system.

A damage index can be based on hysteretic energy. For example, for EPP systems, Cosenza, et al. (1993) and Fajfar (1992) used:

$$DI_H = [E_H/(F_y u_y)] / (\mu_{mon} - 1) = (\mu_H - 1) / (\mu_{mon} - 1) \quad (4a)$$

For a general force-deformation relationship, the above DI can be rewritten (Cosenza, et al., 1993):

$$DI_H = E_H / E_{Hmon} \quad (4b)$$

where E_{Hmon} is hysteretic energy capacity of the system under monotonically increasing deformation.

A combination of maximum deformation response and hysteretic energy dissipation was proposed by Park and Ang (1985):

$$DI_{PA} = (u_{max} / u_{mon}) + \beta E_H / (F_y u_{mon}) \quad (5)$$

where $\beta \geq 0$ is a constant, which depends on structural characteristics. DI_{PA} has been calibrated against numerous experimental results and field observations in earthquakes (e.g., Park et al., 1987; Ang and de Leon, 1994). $DI_{PA} < 0.4$ to 0.5 has been reported as the limit of repairable damage (Ang and de Leon, 1994). Cosenza, et al. (1993) reported that experimental-based values of β have a median of 0.15 and for this value, DI_{PA} correlates well with the results of other damage models proposed by Banon and Veneziano (1982) and Krawinkler and Zohrei (1983). DI_{PA} has drawbacks; two of them will be mentioned here. First, for elastic response, when $E_H=0$ and the damage index is supposed to be zero, the value of DI_{PA} will be greater than zero. The second disadvantage of DI_{PA} is that it does not give the correct result when the system is under monotonic deformation. Under such a deformation, if the maximum deformation capacity (u_{mon}) is reached, the value of the damage index is supposed to be 1.0, i.e., an indication of potential of failure. However, as it is evident from (5), DI_{PA} results in a value greater than 1.0. Chai et al. (1995) modified DI_{PA} to correct the second deficiency of DI_{PA} , as mentioned above; however, the first deficiency of DI_{PA} was not corrected. Despite its drawbacks, DI_{PA} has been extensively used for different applications. This is, in part, due to its simplicity and its extensive calibration against experimentally observed seismic structural damage.

Improved Damage Indices

Bozorgnia and Bertero (2001) introduced two improved damage indices for a generic inelastic SDOF system. These damage indices are as follows:

$$DI_1 = [(1 - \alpha_1) (\mu - \mu_e) / (\mu_{mon} - 1)] + \alpha_1 (E_H / E_{Hmon}) \quad (6)$$

$$DI_2 = [(1 - \alpha_2) (\mu - \mu_e) / (\mu_{mon} - 1)] + \alpha_2 (E_H / E_{Hmon})^{1/2} \quad (7)$$

where,

$$\mu = u_{max} / u_y = \text{Displacement ductility} \quad (8a)$$

$$\mu_e = u_{elastic} / u_y = \text{Maximum elastic portion of deformation} / u_y \quad (8b)$$

= 1 for inelastic behavior; and

= μ if the response remains elastic

μ_{mon} is monotonic displacement ductility capacity, E_H is hysteretic energy demanded by the earthquake ground motion, E_{Hmon} is hysteretic energy capacity under monotonically increasing lateral deformation, and $0 \leq \alpha_1 \leq 1$ and $0 \leq \alpha_2 \leq 1$ are constants. Using the definition of hysteretic ductility μ_H (Mahin and Bertero, 1976; and 1981) given in equation (3) for both earthquake and monotonic deformations, the new damage indices can be rewritten as:

$$DI_1 = [(1 - \alpha_1) (\mu - \mu_e) / (\mu_{mon} - 1)] + \alpha_1 (\mu_H - 1) / (\mu_{Hmon} - 1) \quad (9)$$

$$DI_2 = [(1 - \alpha_2) (\mu - \mu_e) / (\mu_{mon} - 1)] + \alpha_2 [(\mu_H - 1) / (\mu_{Hmon} - 1)]^{1/2} \quad (10)$$

For the special case of elastic-perfectly-plastic (EPP) systems:

$$E_{Hmon} = F_y (u_{mon} - u_y) \text{ and } \mu_{Hmon} = \mu_{mon} \quad (11)$$

$$DI_1 = [(1 - \alpha_1) (\mu - \mu_e) / (\mu_{mon} - 1)] + \alpha_1 (E_H / F_y u_y) / (\mu_{mon} - 1) \quad (12)$$

$$DI_2 = [(1 - \alpha_2) (\mu - \mu_e) / (\mu_{mon} - 1)] + \alpha_2 [(E_H / F_y u_y) / (\mu_{mon} - 1)]^{1/2} \quad (13)$$

Few characteristics of the improved damage indices are listed below:

- 1) If the response remains elastic, i.e., when there is no significant damage, then $\mu_e = \mu$ and $E_H = 0$, and consequently both DI_1 and DI_2 will become zero. This is a characteristic expected for any damage index.
- 2) Under monotonic lateral deformation if $u_{max} = u_{mon}$, the damage indices will be unity. This is true for a general force-deformation relationship.
- 3) If $\alpha_1 = 0$ and $\alpha_2 = 0$, damage indices DI_1 and DI_2 (equations 6 and 7) will be reduced to a special form given in equation (1). In this special case, the damage index is assumed to be only related to the maximum *plastic* deformation.
- 4) If $\alpha_1 = 1$ and $\alpha_2 = 1$, damage indices DI_1 and DI_2 will be only related to the hysteretic energy dissipation E_H . Specifically, in this case, damage index DI_1 will be reduced to a special form given in equation (4b). If additionally the force-deformation relationship is EPP, damage index DI_1 given in (12) will be reduced to a special form given in equation (4a).
- 5) Equivalent hysteretic velocity V_H (Uang and Bertero, 1988) was defined as:

$$V_H = (2 E_H / M)^{1/2} \quad (14)$$

where M is the mass of the system. It is evident from the definition of DI_2 given in (7) that DI_2 is related to the normalized equivalent hysteretic velocity. If V_H spectrum is already available, DI_2 can be easily generated.

Development of Damage Spectra

As mentioned before, damage spectrum of a recorded ground motion represents variation of a damage index versus structural period for a series of SDOF systems. Once a damage index, such as DI_1 and DI_2 , is defined, damage spectrum can be constructed. The steps involved in developing the damage spectrum are summarized in Figure 1.

Examples of damage spectra are presented in Figure 2. This figure shows damage spectra for the 1940 Imperial Valley earthquake recorded at El Centro, and for the Northridge earthquake recorded at Sylmar County Hospital. For this figure, the following characteristics were used: viscous damping $\gamma=5\%$; EPP force-displacement relationship; yield strength was based on elastic spectrum of UBC-97 (without near-source factors) reduced by $R_d=3.4$; also $\mu_{mon}=10$, $\alpha_1=0.269$, $\alpha_2=0.302$ were used. These values for α_1 and α_2 are based on an analysis of the Northridge earthquake records, as explained below. Computer program Nonspec (Mahin and Lin, 1983) was employed to compute the basic response parameters such as displacement ductility and hysteretic energy demands. DI_1 and DI_2 were then computed according to equations (12) and (13). The damage spectra for periods longer than 0.5 sec are plotted in Figure 2. For the structures with

shorter periods, generally larger over-strength factor and μ_{mon} should be used. The contrast between the two damage spectra presented in Figure 2 is an evidence of very different damage potentials of these two ground motion records for the SDOF systems considered.

As mentioned previously, DI_{PA} has been already calibrated against numerous experimental and field cases. However, because of its deficiencies, it is not reliable at its low and high values. Thus, in the intermediate range of the damage index, a comparison between values of DI_1 with those of DI_{PA} can result in an estimate for α_1 . Hence, the following procedure was used to estimate α_1 : ductility and hysteretic energy spectra and DI_{PA} were computed at 20 structural periods ranging from 0.1 to 4.0 seconds using 220 horizontal ground acceleration records of the Northridge earthquake. Then coefficient α_1 was determined through regression analyses, i.e., by comparing values of DI_1 with those of DI_{PA} (for $0.2 < DI_{PA} < 0.8$). A similar process was repeated to estimate coefficient α_2 in DI_2 . The same procedure was also carried out using 176 horizontal acceleration records of the 1992 Landers, California, earthquake. The computed α_1 and α_2 coefficients using the ground motion records of the Northridge and Landers earthquakes are listed in Table 1. Subsets of the results of the regression analyses for the Northridge earthquake are also graphically presented in Figure 3.

Effects of Strong-Motion Duration

Experimental studies have demonstrated that failures of structural members and systems are influenced by the number of inelastic cycles of response (e.g., Bertero, et al., 1977). In other words, structural systems generally become more vulnerable if they go through repeated cycles of inelastic motions. This generally occurs when the structure is subjected to a strong ground motion with a long duration. Hence, in quantifying damage potential of the recorded ground motion it is desirable to include the effects of strong ground motion duration.

Hysteretic energy E_H through its definition (e.g., Uang and Bertero, 1981) is a cumulative quantity. More cycles of inelastic deformations correspond to a larger value for the hysteretic energy dissipation. Thus, the effects of repeated cycles of inelastic response and strong-motion duration are reflected in E_H . Hence, in the damage indices that include hysteretic energy terms, the effects of repeated cycles of inelastic deformations and strong-motion duration are also included. An example of the duration effect on E_H and damage spectrum is shown in Figure 4.

In 1999 two major earthquakes occurred in Turkey: (1) on August 17, 1999 an earthquake of magnitude M_s 7.8; and (2) on November 12, 1999 another major earthquake of magnitude 7.5 (EERI, 2000). For both events, the ground accelerations were recorded at Duzce station. Figure 4 shows the ground accelerations recorded in these two events, with 10 seconds of zero ground acceleration added in between. Time variation of the hysteretic energy demand is also plotted in Figure 4. Damage spectra of the first and second events individually, as well as the damage spectrum of the combined acceleration records were computed and presented in Figure 4. The results shown in this figure are based on the same basic parameters as used in Figure 2 (except with $\mu_{\text{mon}}=8$, $a_1=0.286$ and include near-source factors). Displacement ductility spectra are also plotted in Figure 4. As it is expected, the time variation of the hysteretic energy clearly shows that E_H incorporates the cumulative effects due to the strong-motion duration. Because the

damage spectrum includes E_H spectrum (see Figure 1), the damage spectrum is also influenced by the cumulative effects. Such an effect, however, is not included in the displacement ductility spectra. It should be noted that the effects of the sequence, and therefore the history, of different hysteretic loops are not considered in proposed damage spectra.

Attenuation of Damage Spectra

Once damage spectral ordinates for numerous ground motion records are computed, it is possible to evaluate the attenuation of damage spectra. Such an attenuation model can be used to estimate the variation of the damage spectral ordinates with site-to-source distance. To demonstrate the concept, attenuation of the damage spectral ordinates for the Northridge earthquake was computed. First, damage spectra for the horizontal accelerations recorded at alluvial sites during the Northridge earthquake were calculated for the same set of parameters as used for Figure 2. Then, regression analyses were performed on the following attenuation model:

$$\ln(DI_1) = a + d \ln [R^2 + c^2]^{1/2} + e \quad (15)$$

where R is the closet distance from the site to the surface projection of the fault plane, e is a random error, and a , c , and d are the regression parameters to be computed. Site soil conditions at the recording stations and site-to-source distances were taken from a comprehensive ground motion database compiled by Campbell and Bozorgnia (2000) and Bozorgnia et al. (1999). The distance scaling of the damage spectral ordinates is shown in Figure 5. The median damage spectra for distances 3, 10, 20, and 40 km from the fault are also plotted in the same figure. It should be noted that the damage spectra shown in Figure 5 are based on the assumption that structural over-strength factor and μ_{mon} are constant over the period range. These factors, however, are possibly higher at short periods (e.g., for low-rise buildings) than those at long periods.

SPATIAL DISTRIBUTION OF VARIOUS PARAMETERS

For any specified structural characteristics and using the recorded ground motions at various recording stations, it is possible to rapidly generate damage spectra and plot their spatial distribution at selected periods. As an example, contours of damage spectral ordinates based on 220 horizontal accelerations recorded during the Northridge earthquake are plotted in Figure 6 for periods 1.0 and 3.0 seconds. For computation of damage spectra, the same basic parameters as Figure 2 were used, except $\mu_{mon}=12$. Also, uniform basic structural characteristics over the area were assumed. Soil conditions at the recording stations were taken from the strong-motion database compiled by Campbell and Bozorgnia (2000) and Bozorgnia et al. (1999). The soil conditions were used to adjust F_y/W of the SDOF system at the recording site (see Figure 1). At each recording station the maximum of the damage spectral ordinates for the two horizontal components was taken. Figure 6 also shows the epicenter of the earthquake and the surface projection of the fault plane. Contour plots for DI_2 (not shown here) are very comparable to those plotted in Figure 6. As mentioned above, this figure is for uniformly distributed structural characteristics in the area, except for the adjustment of F_y/W for the local soil conditions. However, the distribution of the damage spectral ordinates can be modified to incorporate the data from an inventory of the existing structures in the area. For example, for buildings, data on the structural material, structural system, number of stories, age of the structure, etc. can be

approximately translated into the basic structural data needed to generate damage spectra. If a better estimate of the spatial distribution of the basic structural characteristics is used, more realistic contour plots of the damage spectral ordinates can be generated.

Plotted in Figure 6 are also the distributions of the displacement ductility demanded by the recorded ground motion at periods 1.0 and 3.0 seconds. The same basic parameters were used as those for the damage spectral ordinates.

Given the displacement ductility, and consequently the maximum displacement of the SDOF system, interstory drift ratio can be estimated. The following procedure was implemented: First, given the specified structural period, building height was estimated using the period-height relationship suggested by Goel and Chopra (1997) for reinforced concrete moment-resisting frames. For the purpose of estimating the drift, the smaller height estimated by the period formulas, was used. Then, the tentative guidelines provided by SEAOC (1999), Appendix I, were used to approximately estimate the interstory drift ratio. Figure 7 shows the contour plots of interstory drift demanded by the recorded ground motion.

Equivalent hysteretic velocity V_H (equation 14) is directly related to the hysteretic energy dissipation demanded by the recorded ground motion. As mentioned before, the effects of cycles of inelastic response and strong-motion duration are included in V_H , as well as in the damage spectra. As an example, distribution of V_H spectral ordinates at a period of 1.0 second is also shown in Figure 7.

Housner spectrum intensity (Housner, 1952; and 1975) for 5% damping was also computed for the horizontal accelerations recorded in the Northridge earthquake. At each recording station, maximum of the spectrum intensities of the two horizontal components was taken. Spatial distribution of the spectrum intensity is also shown in Figure 7.

Drift spectrum (Iwan, 1997) is a measure of maximum interstory drift ratio using a linear shear-beam model. Contours of drift spectral ordinates at the base level of the structure at periods 1.0 and 3.0 seconds for 5% damping ratio are shown in Figure 8. Computation of the drift spectra requires ground velocity and displacement histories (Iwan, 1997). To avoid any distortion of long-period information, the available velocity and displacement histories of the near-source records without band-pass filtering were used (Iwan, 1995). This may be one possible source of the difference between the drift plots in Figures 7 and 8.

Selected results for the Landers earthquake are also shown in Figure 9. This figure shows the damage spectral ordinates DI_1 , with the same SDOF characteristics as used in Figure 2, except for $\mu_{mon}=12$, and $a_1=0.316$. Again, a uniform distribution of structural characteristics in the area was used. The fault trace and the epicenter of the earthquake are also mapped in the figure. Displacement ductility and interstory drift ratio at period 1.0 second are also presented in this figure. For the computation of the interstory drift ratio, the same procedure was used as that for Figure 7.

Various contour plots in Figures 6-9 reveal information about different measures of the severity of the recorded ground motion at different locations. Some of them also reveal more information about performance of a set of simple structural models subjected to the recorded ground motion. One obvious advantage of the spectral damage contour plots is that they conveniently represent normalized values. For example, compare the contour plots of the damage spectral ordinates with displacement ductility demands. In order to compare them, ranges of

ductility values need to be correlated to various structural performance descriptions (such as “operational”, “life safe”, “near collapse”, etc.). Using, for example, such a tentative correlation given in SEAOC (1999), Appendix I, contour plots of the damage spectra and displacement ductility are generally consistent. However, the damage spectral plots, representing a normalized quantity, are more convenient for post-earthquake applications. Additionally, as mentioned before, they include more features of the inelastic response than most of the other parameters considered.

COMPARISON OF PARAMETERS FOR SPECIFIC CASES

Ground shaking and damage parameters considered were compared for specific cases. This section presents a summary of the comparison.

Van Nuys seven-story hotel is an instrumented building which experienced major structural damage during the Northridge earthquake (California Seismic Safety Commission, 1996; Moehle, et al., 1997). The structure is a seven-story reinforced concrete frame building constructed in 1966 and no seismic retrofit work was performed prior to the Northridge earthquake. The details of the building are reported by California Seismic Safety Commission (1996), and Moehle, et al. (1997). Structural damage was primarily restricted to the longitudinal perimeter frames, and the damage included column shear failures, and immediately after the earthquake the building was “red tagged”. Various ground motion and damage parameters were computed using the recorded accelerations at ground level in EW direction. For the damage spectrum, basic structural characteristics were taken from the previous detailed analyses (California Seismic Safety Commission, 1996; Moehle, et al., 1997). In a reverse process, having assigned a damage index of 0.8 (for a “near collapse” damage state), value of μ_{mon} was estimated for different values of a_1 and a_2 . Summary of the results are given in Table 2. A range of 4.2 to 5.6 was computed for μ_{mon} . Compared with the results of the previous detailed nonlinear analyses, this seems a reasonable range. Computed drift ratio of 1.3%, estimated by both inelastic SDOF and drift spectrum analyses, is also within the range of 1.2 to 1.9% based on the recorded motions of the building. This example shows that it is possible to estimate the damage spectrum with a good accuracy, if the needed basic structural characteristics are accurately estimated.

Another case study is a set of 17 low-rise (1 to 3-story) ductile moment-resisting reinforced concrete frame buildings constructed between 1979 and 1990. These buildings were affected by the Northridge earthquake. Singhal and Kiremidjian (1996) assigned damage indices (DIs) to these buildings. These assigned DIs were based on the reported repair costs, not rehabilitation costs, and not based on direct field observations. The assigned DIs are very low -- an indication that the damage to these buildings was not severe. The highest reported DI is 0.26 for building #17 located at about 1.8 km from the Rinaldi Receiving Station (RRS). For each building, the closest free-field recording station located at the same general soil category was identified in the present study. Using the recorded motions various shaking and damage parameters were computed. Regression analyses were performed to compare the computed and assigned values of the damage indices, and to estimate μ_{mon} . The results, although very scattered, all indicate that in order to obtain the very low assigned DIs, the values of μ_{mon} and/or over-strength factor should be very high. This is conceptually consistent with the general understanding that the available global ductility and over-strength factor for low-rise ductile buildings are high. Another

observation is that the recorded motion at RRS, which is close to building #17, is a very strong motion by almost all measures. For example, the peak horizontal ground acceleration (PGA) is 0.84g, peak ground velocity (PGV) is 159 cm/sec (Iwan, 1997), elastic spectral ordinates between periods 0.3-0.5 sec exceed about 1.7g, spectrum intensity for 5% damping is 456cm, and drift spectrum for 5% damping at 0.3-0.5 sec is between 1.5 and 2.26%. However, as mentioned before, the assigned damage index is low (Singhal and Kiremidjian, 1996) indicating no significant damage.

Consider, for example, spectrum intensity at RRS (456 cm) and that at the Van Nuys seven-story building (174 and 230 cm, for the motion at the building base and free-field record, respectively). Purely based on this parameter, more damage may be expected at the site of building #17 than the Van Nuys seven-story building. This is due to the fact that strength, deformation and energy dissipation capacities of the structures are important factors in controlling the response, and therefore the damage. These factors, however, do not have any influence on the computed values of, e.g., elastic spectral ordinates or spectrum intensity. Hence, such parameters alone cannot accurately predict the observed damage.

CONCLUDING REMARKS

In this study several ground shaking, response and damage parameters were computed and examined. Two improved damage spectra and their characteristics were also examined. The parameters considered in this study can be classified into the following categories:

- *Parameters that are purely measures of free-field ground motion.* These include PGA and PGV, which are amongst the most important parameters measuring severity of the ground motion. However, they are independent of any data about the behavior of structural systems. Therefore, besides their other limitations, these parameters *alone* have limited capabilities to accurately predict damage.
- *Parameters that are related to the elastic response of SDOF and shear-beam models.* These include elastic spectral ordinates, spectrum intensity, and drift spectrum. Although these are also very important measures and their applications have been extensive, they do not include effects of inelastic structural response and repeated cycles of inelastic deformations, which are generally associated with damage.
- *Inelastic response spectra in the forms of displacement ductility, interstory drift ratio, and strength spectra.* These parameters reveal some fundamental features of inelastic response; however, the effects of number of cycles of inelastic response and duration of strong ground motion are not included.
- *Spectrum of hysteretic energy dissipation due to plastic deformations, and its associated equivalent hysteretic velocity spectra.* These parameters include some fundamental features of inelastic response as well as the effects of repeated cycles of inelastic deformations and strong ground motion duration. However, in order to use these parameters for rapid damage assessments and post-earthquake applications, they have to be normalized with the energy dissipation capacity of the structure.
- *Damage spectrum.* It is based on normalized response quantities of a series of inelastic SDOF systems. The improved damage spectra presented here are based on promising damage indices (DIs). The proposed damage spectra explicitly satisfy two important conditions: They

SMIP01 Seminar Proceedings

will be zero if the response remains elastic, i.e., no significant damage is expected; and will be unity when the maximum deformation capacity is reached under monotonically increasing lateral deformation. Larger damage spectral ordinates conceptually correspond to larger damage.

Another characteristic of the proposed damage spectra is that by varying a coefficient (a_1 in DI_1 , or a_2 in DI_2), they are reduced to the commonly used normalized hysteretic energy and displacement ductility spectra. Also, the damage spectra, in their general form, are influenced by the repeated cycles of inelastic deformations and strong-motion duration. Although the proposed DIs may be further improved to include other features of inelastic response, they are more reliable indices than other commonly used DIs such as DI_{PA} .

The proposed damage spectra can be used to quantify the damage potential of the recorded ground motion and relate that to seismic structural performance categories. They are also effective quantities for post-earthquake applications and rapid identification of the damaged areas based on the recorded ground motions and the type of construction. Utilization of an up-to-date inventory of existing structures enhances the reliability of spatial distribution of the damage spectra.

ACKNOWLEDGEMENTS

This study was supported by the California Department of Conservation, Division of Mines and Geology, Strong Motion Instrumentation Program, Contract 1099-733. The support is gratefully acknowledged. The authors are grateful to Dr. Ken Campbell for providing soil and ground motion information at the sites of low-rise concrete buildings affected by the Northridge earthquake, and Dr. Ajay Singhal for extracting the construction dates of the same set of buildings. The authors also wish to thank Prof. Bill Iwan for providing the routine for computation of the drift spectrum, and Prof. Mustafa Erdik for supplying the ground motion records at Duzce, Turkey. Constructive comments by the members of California Strong-Motion Instrumentation Advisory Subcommittees are fully appreciated.

REFERENCES

- Ang, A.H-S., and D. de Leon (1994). "Reliability and response control of R/C buildings," *Proceedings, ASCE Structures Congress XII*, Vol. 2, pp. 1593-1599.
- Arias, A. (1970). "A measure of earthquake intensity," in *Seismic Design for Nuclear Power Plants*, R.J. Hansen, Editor, MIT Press.
- Banon, H., and D. Veneziano (1982). "Seismic safety of reinforced concrete members and structures," *Earthquake Engineering and Structural Dynamics*, Vol.10, pp.179-193.
- Bertero, V.V., S.A. Mahin, and R.A. Herrera (1978). "Aseismic design implications of near-fault San Fernando earthquake records," *Earthquake Engineering and Structural Dynamics*, Vol.6, pp.31-42.
- Bertero, V.V., E.P. Popov, T.Y. Wang, and J. Vallenias (1977). "Seismic design implications of hysteretic behavior of reinforced concrete structural walls," *Proceedings, 6th World Conference on Earthquake Engineering*, India, Vol. II, pp.1898-1904.
- Bertero, V.V., and C-M Uang (1992). "Issues and future directions in the use of an energy approach for seismic-resistant design of structures," in *Nonlinear Seismic Analysis and*

SMIP01 Seminar Proceedings

- Design of Reinforced Concrete Buildings*, Edited by P. Fajfar and H. Krawinkler, pp. 3-22.
- Bolt, B.A. (1973). "Duration of strong ground motion," *Proceedings, 5th World Conference on Earthquake Engineering*, Rome, pp. 1304-1313.
- Bozorgnia, Y., and V.V. Bertero (2001). "Evaluation of damage potential of recorded earthquake ground motion," *96th Annual Meeting of Seismological Society of America*, San Francisco, CA, April 17-21, 2001.
- Bozorgnia, Y., K.W. Campbell, and M. Niazi, M.(1999). "Vertical ground motion: Characteristics, relationship with horizontal component, and building code implications," *Proceedings, SMIP99 Seminar on Utilization of Strong-Motion Data*, San Francisco, pp. 23-49.
- California Seismic Safety Commission (1996). "1994 Northridge Earthquake Building Case Studies Project." *Report SSC 94-06*, Proposition 122, Product 3.2, State of California Seismic Safety Commission, Sacramento, CA.
- Campbell, K.W., and Y. Bozorgnia (2000). "New empirical models for predicting near-source horizontal, vertical, and V/H response spectra: Implications for design," *Proceedings, 6th International Conference on Seismic Zonation*, Palm Springs, CA.
- Chai, Y.H., K.M. Romstad, and S.M. Bird (1995). "Energy-based linear damage model for high-intensity seismic loading," *ASCE Journal of Structural Engineering*, Vol. 121, No.5, pp. 857-864.
- Cosenza, E., G. Manfredi, and R. Ramasco (1993). "The use of damage functionals in earthquake engineering: A comparison between different methods," *Earthquake Engineering and Structural Dynamics*, Vol. 22, pp.855-868.
- EERI (2000). "1999 Kocaeli, Turkey, earthquake reconnaissance report," *Earthquake Spectra*, Supplement to Vol. 16.
- Fajfar, P. (1992). "Equivalent ductility factors, taking into account low-cycle fatigue," *Earthquake Engineering and Structural Dynamics*, Vol. 21, pp.837-848.
- Goel, R.K., and A.K. Chopra (1997). "Period formulas for moment-resisting frame buildings." *ASCE Journal of Structural Engineering*, Vol. 123, No. 11, pp. 1454-1461.
- Housner, G.W. (1952). "Spectrum intensities of strong-motion earthquakes," *Proceedings, Symposium on Earthquake and Blast Effects on Structures*, Edited by C.M. Duke and M. Feigen.
- Housner, G.W. (1975). "Measures of severity of earthquake ground shaking," *Proceedings, U.S. National Conference on Earthquake Engineering*, Ann Arbor, Michigan, pp.25-33.
- Iwan, W.D. (1995). "Drift demand spectra for selected Northridge sites," *Report No. 95-07*, Earthquake Engineering Research Lab., California Inst. of Technology.
- Iwan, W.D. (1997). "Drift spectrum: Measure of demand for earthquake ground motions," *ASCE Journal of Structural Engineering*, Vol.123, No.4, pp.397-404.
- Krawinkler, H., and M. Zohrei (1983). "Cumulative damage in steel structures subjected to earthquake ground motion," *Computers and Structures*, Vol. 16, pp.531-541.

SMIP01 Seminar Proceedings

- Mahin, S.A., and V.V. Bertero (1976). "Problems in establishing and predicting ductility in aseismic design," *Proceedings, International Symposium on Earthquake Structural Engineering*, St. Luis, Missouri, August 1976, pp 613-628.
- Mahin, S.A., and V.V. Bertero (1981). "An evaluation of inelastic seismic design spectra," *ASCE Journal of Structural Division*, Vol. 107, No. ST9, pp. 1777- 1795.
- Mahin, S.A., and J. Lin (1983). "Construction of inelastic response spectra for single-degree-of-freedom systems" *Report UCB/EERC-83/17*, Earthquake Engineering Research Center, University of California, Berkeley.
- Moehle, J.P., Y.R. Li, A. Lynn, and J. Browning (1997). "Performance assessment for a reinforced concrete frame building," *Proceedings, NEHRP Conference and Workshop on Research on the Northridge, California Earthquake of January 17, 1994*, Vol. III-A, pp.140-156.
- Newmark, N.M., and W.J. Hall (1982). "Earthquake spectra and design," *Monograph*, Earthquake Engineering Research Institute (EERI).
- Park, Y.J., and A.H-S. Ang (1985). "Mechanistic seismic damage model for reinforced concrete," *ASCE Journal of Structural Engineering*, Vol. 111, No.4, pp.722-739.
- Park, Y.J., A.H-S. Ang, and Y.K. Wen (1987). "Damage-Limiting aseismic design of buildings," *Earthquake Spectra*, Vol. 3, No.1, pp.1-26.
- Powell, G.H. and R. Allahabadi (1988). "Seismic damage prediction by deterministic methods: Concepts and procedures," *Earthquake Engineering and Structural Dynamics*, Vol. 16, pp.719-734.
- SEAOC (1999). "Recommended Lateral Force Requirements and Commentary," *Report*, Seismology Committee, Structural Engineers Association of California, 7th Edition.
- Singhal, A., and A.S. Kiremidjian (1996). "A method for earthquake motion-damage relationships with application to reinforced concrete frames." *Report No. 119*, The John A. Blume Earthquake Engineering Center, Stanford University.
- Trifunac, M.D., and A.G. Brady (1975). "A study on the duration of strong earthquake ground motion." *Bulletin of Seismological Society of America*, Vol. 65, No. 3, pp.581-626.
- Uang, C-M, and V.V. Bertero (1988). "Implications of recorded earthquake ground motions on seismic design of building structures," *Report No. UCB/EERC-88/13*, Earthquake Engineering Research Center, University of California, Berkeley.
- Uang, C-M, and V.V. Bertero (1990). "Evaluation of seismic energy in structures," *Earthquake Engineering and Structural Dynamics*, Vol. 19, pp.77-90.
- Uniform Building Code* (1997). International Conference of Building Officials, Whittier, CA, Volume 2.
- Wald, D., J., V. Quitoriano, T.H. Heaton., H. Kanamori, C.W. Scrivner, and C.B. Worden (1999). "TriNet "ShakeMaps": Rapid generation of peak ground motion and intensity maps for earthquakes in southern California," *Earthquake Spectra*, Vol. 15, No.3, pp.537-555.

SMIP01 Seminar Proceedings

Table 1—Results of Regression Analyses to Estimate a_1 and a_2

β	μ_{mon}	a_1 Northridge EQ	a_2 Northridge EQ	a_1 Landers EQ	a_2 Landers EQ
0.10	8	0.206	0.273	0.238	0.280
0.15	8	0.286	0.332	0.316	0.331
0.20	8	0.364	0.385	0.378	0.380
0.10	10	0.185	0.243	0.231	0.245
0.15	10	0.269	0.302	0.296	0.297
0.20	10	0.350	0.354	0.357	0.344

Table 2—Summary of the Recorded and Computed Data, Van Nuys Seven-Story Hotel, Northridge Earthquake

Peak Accel. (g)	Elastic Spectrum (g) at 1.5 sec	Damage Spectrum at 1.5 sec	μ_{mon}	Interstory Drift Ratio (%)*	Rel. Roof Disp. / Bldg Height (%) Based on Recorded Bldg Accelerations	Drift: 3 rd -2 nd Flrs (%) Based on Recorded Bldg Accelerations	Drift Spectrum at 1.5 sec (%)**	Spectrum Intensity (cm)***
0.45	0.46	0.8	4.2 – 5.6	1.3	1.2	1.9	1.3	174

(*) Computed using SDOF response

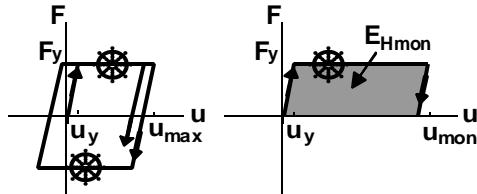
(**) At Base level, for 5% damping

(***) Using the recorded accelerations at the ground level of the building (EW). From free-field contours: 230 cm

DAMAGE SPECTRUM

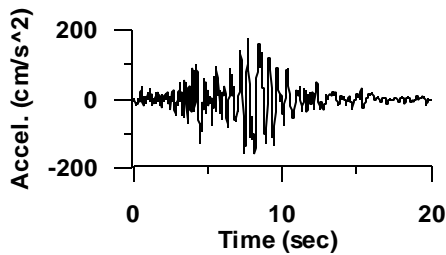
Given: A series of single-degree-of-freedom systems with:

- Period T (sec)
- Damping ratio ξ
- Site soil condition "S" (soil category)
- Strength; specified according to a seismic code: $(F_y/W) = (S_a/g)/R_d$
- A force-deformation relationship:



- E_{Hmon}
("monotonic hysteretic energy capacity")
or, for elastic-perfectly-plastic (EPP):
 μ_{mon} ("monotonic ductility capacity")

Subjected to an earthquake ground acceleration record:



Compute:

- Ductility spectrum (μ)
- Hysteretic energy spectrum (E_H)

Develop Damage Spectrum:

- By combining μ and E_H spectra:

$$DI_1 = [(1 - \alpha_1) (\mu - \mu_e) / (\mu_{mon} - 1)] + \alpha_1 (E_H / E_{Hmon})$$

For special case of EPP systems:

$$DI_1 = [(1 - \alpha_1) (\mu - \mu_e) / (\mu_{mon} - 1)] + \alpha_1 (E_H / F_y \cdot u_y) / (\mu_{mon} - 1)$$

where $0 \leq \alpha_1 \leq 1$ is a constant; $\mu_e = \text{max. elastic deformation} / u_y$

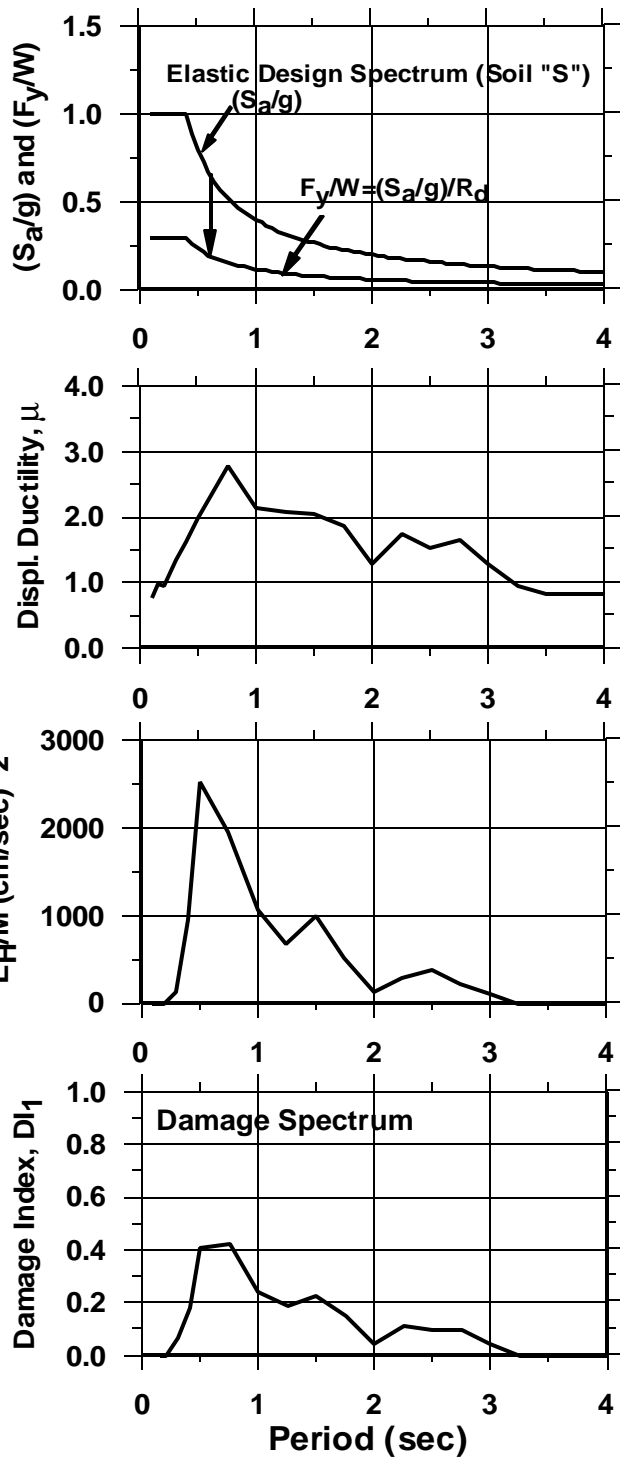


Figure 1: Summary of steps involved in developing *Damage Spectrum*

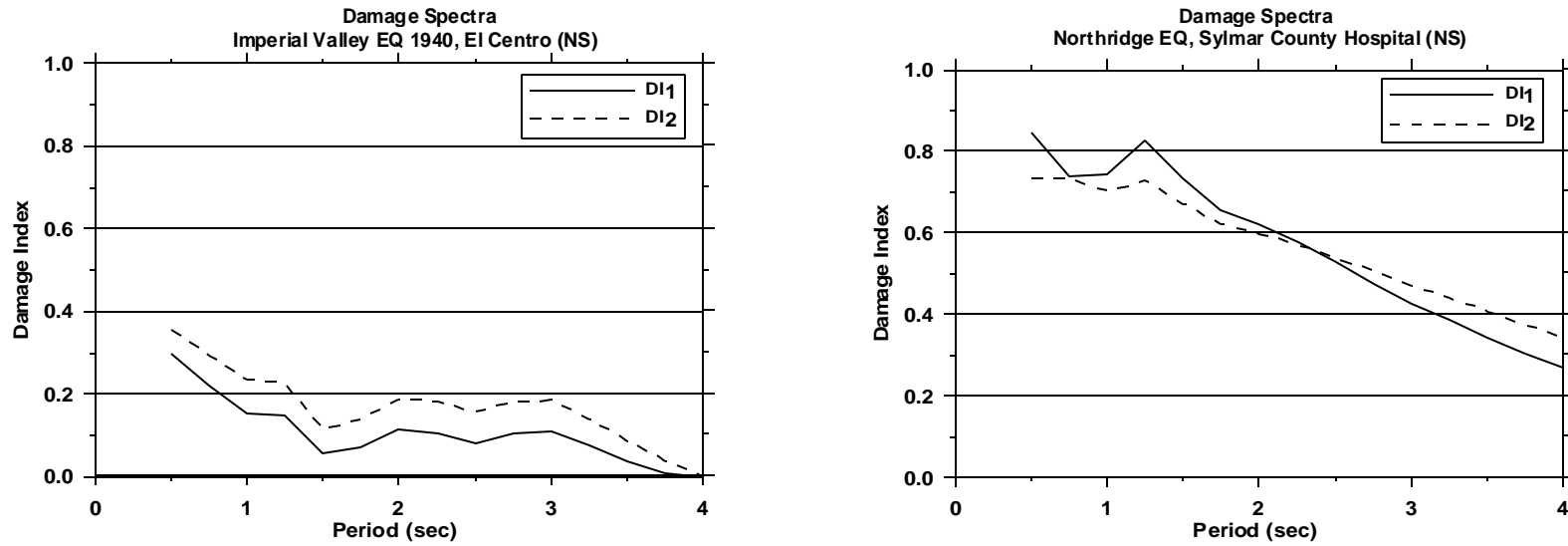


Figure 2: Examples of damage spectra, considering $\xi=5\%$, $\mu_{\text{mon}}=10$, and EPP behavior.

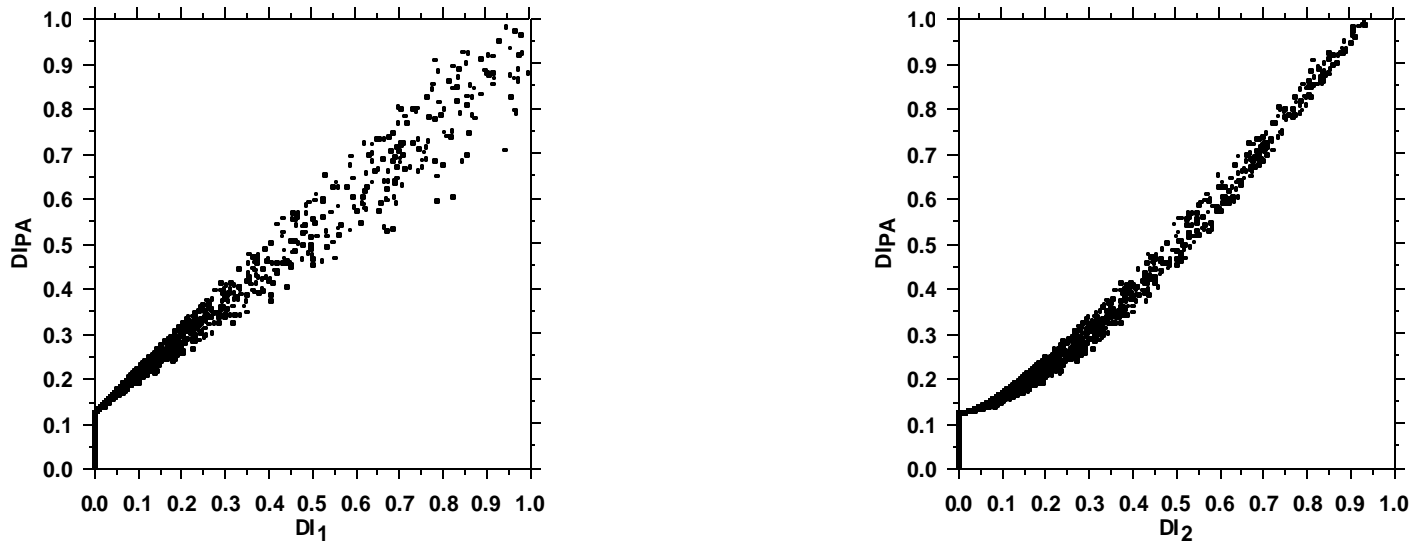


Figure 3: Example of correlation between damage indices (DI_1 , DI_2) and DI_{PA} : Northridge EQ records, with $\beta=0.15$, $\alpha_1=0.286$, $\alpha_2=0.332$, $\mu_{\text{mon}}=8$, $\xi=5\%$.

SMIP01 Seminar Proceedings

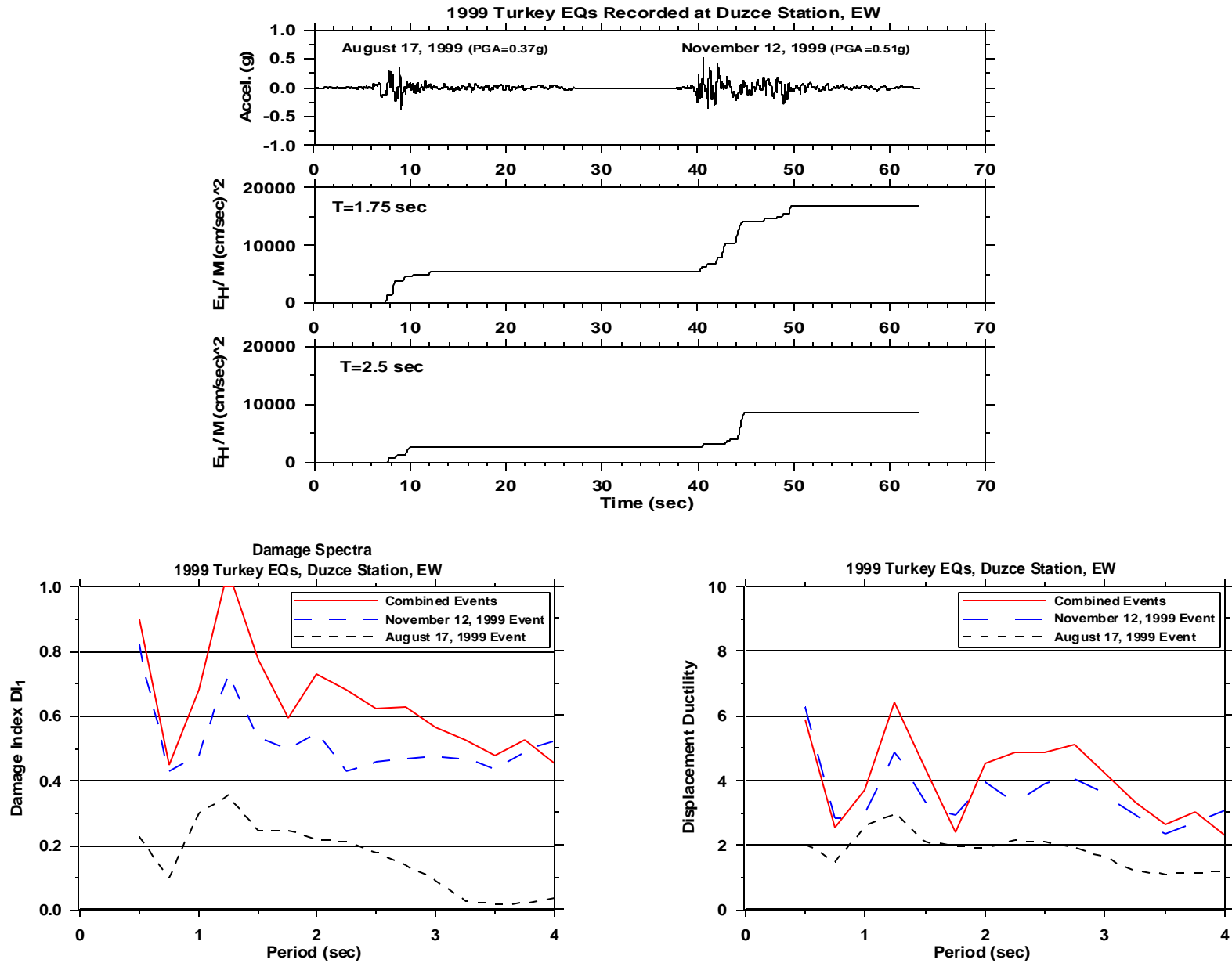


Figure 4: Ground accelerations at Duzce (Turkey); hysteretic energy demands; damage spectra; and displacement ductility.

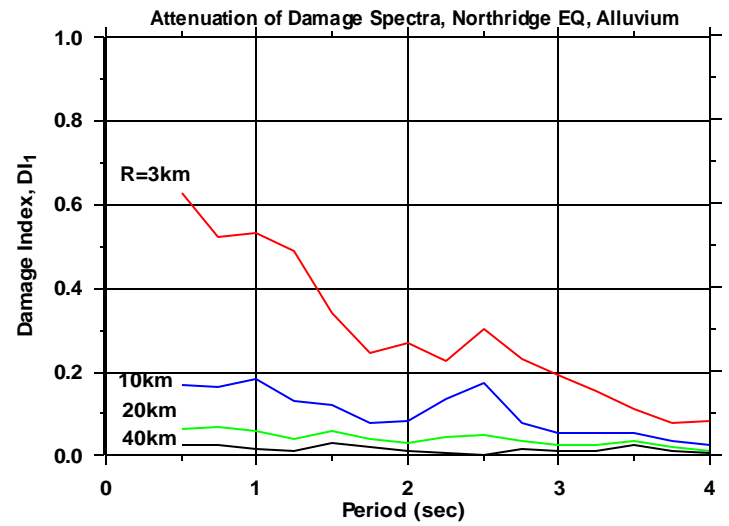
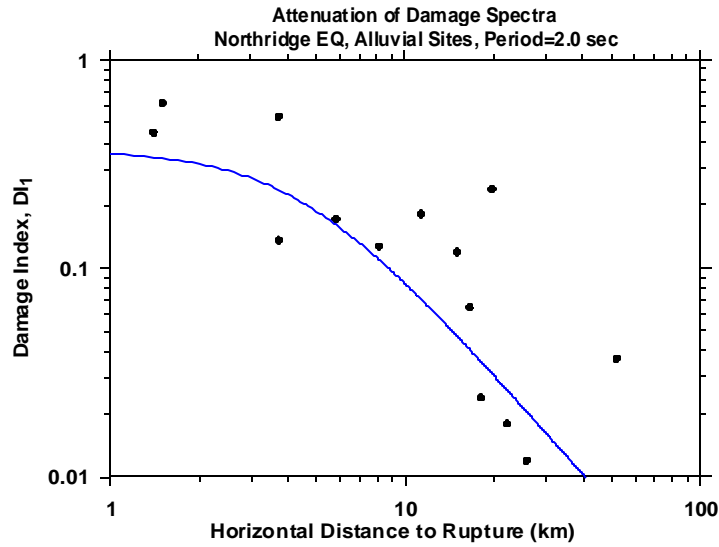
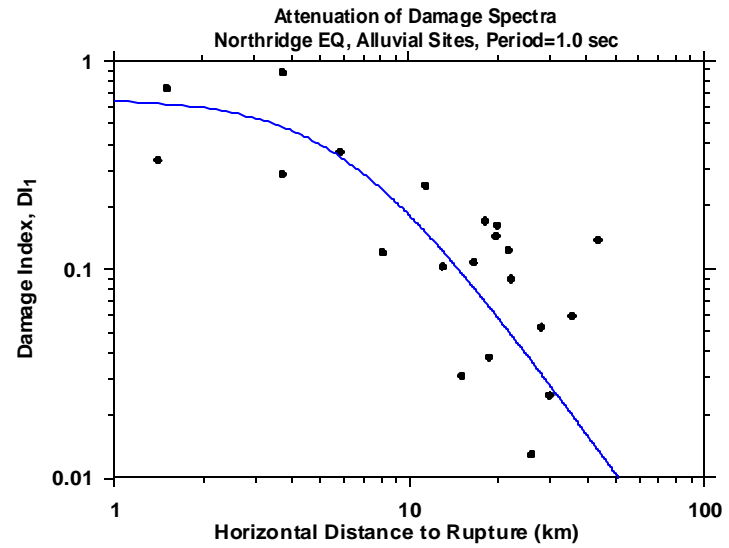
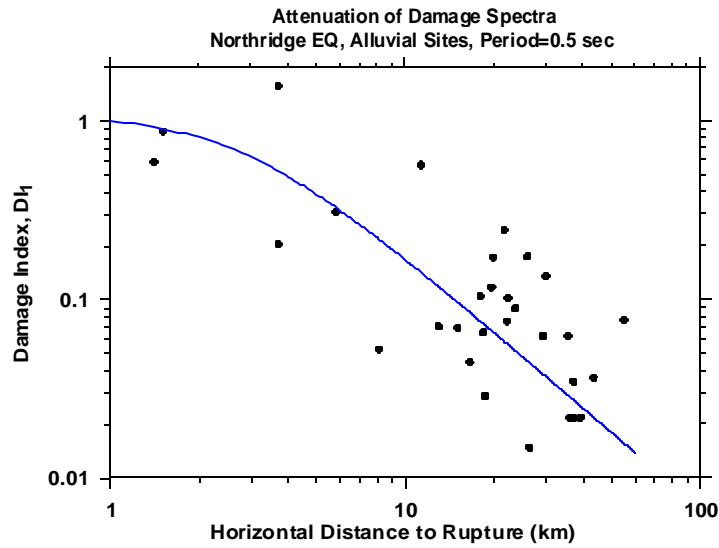


Figure 5: Distance scaling of damage spectral ordinates for the Northridge earthquake at alluvial sites.

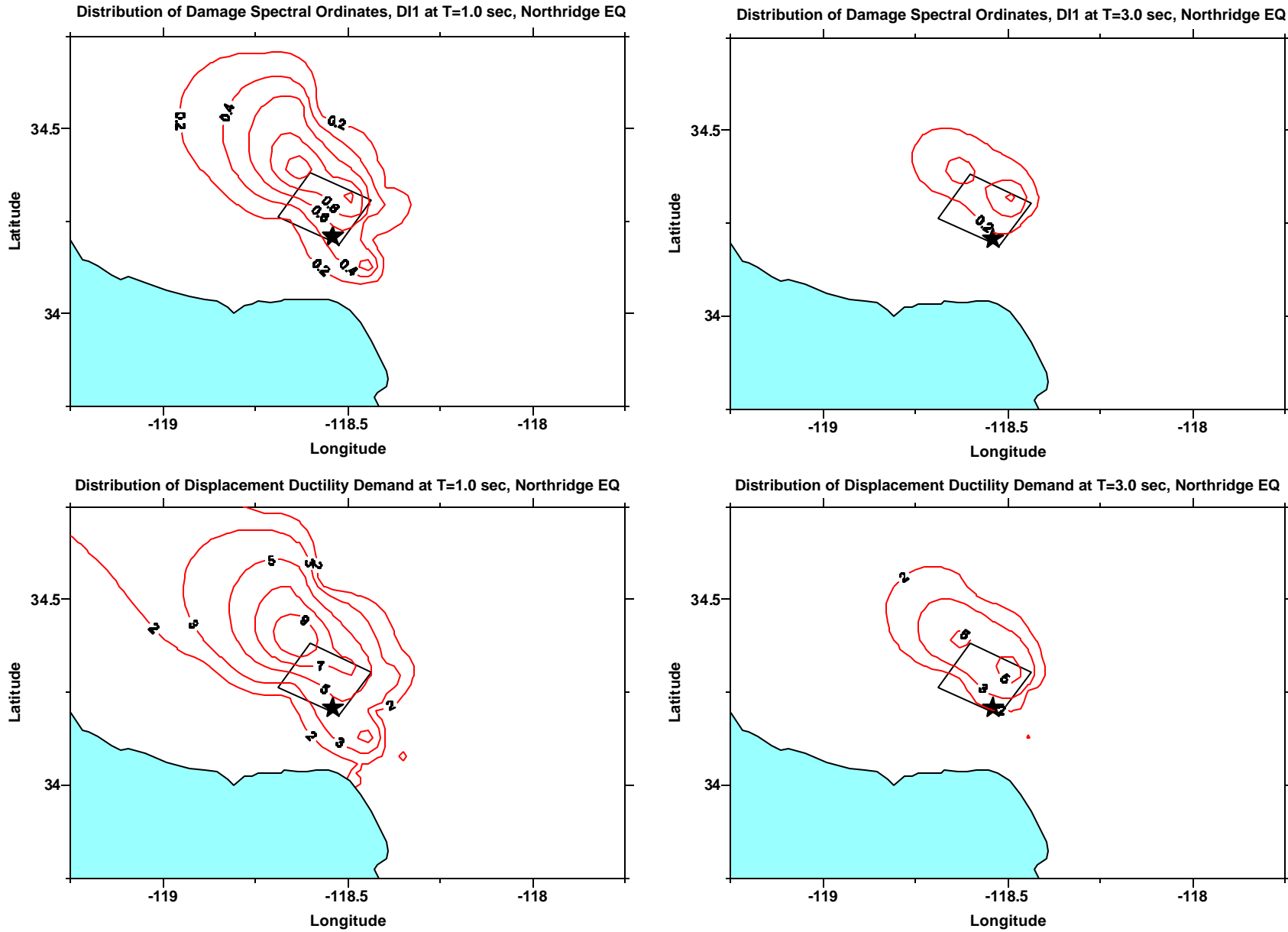


Figure 6: Distribution of damage spectral ordinates and displacement ductility demands of the ground motions recorded during the Northridge earthquake, T=1 and 3 sec.

SMIP01 Seminar Proceedings

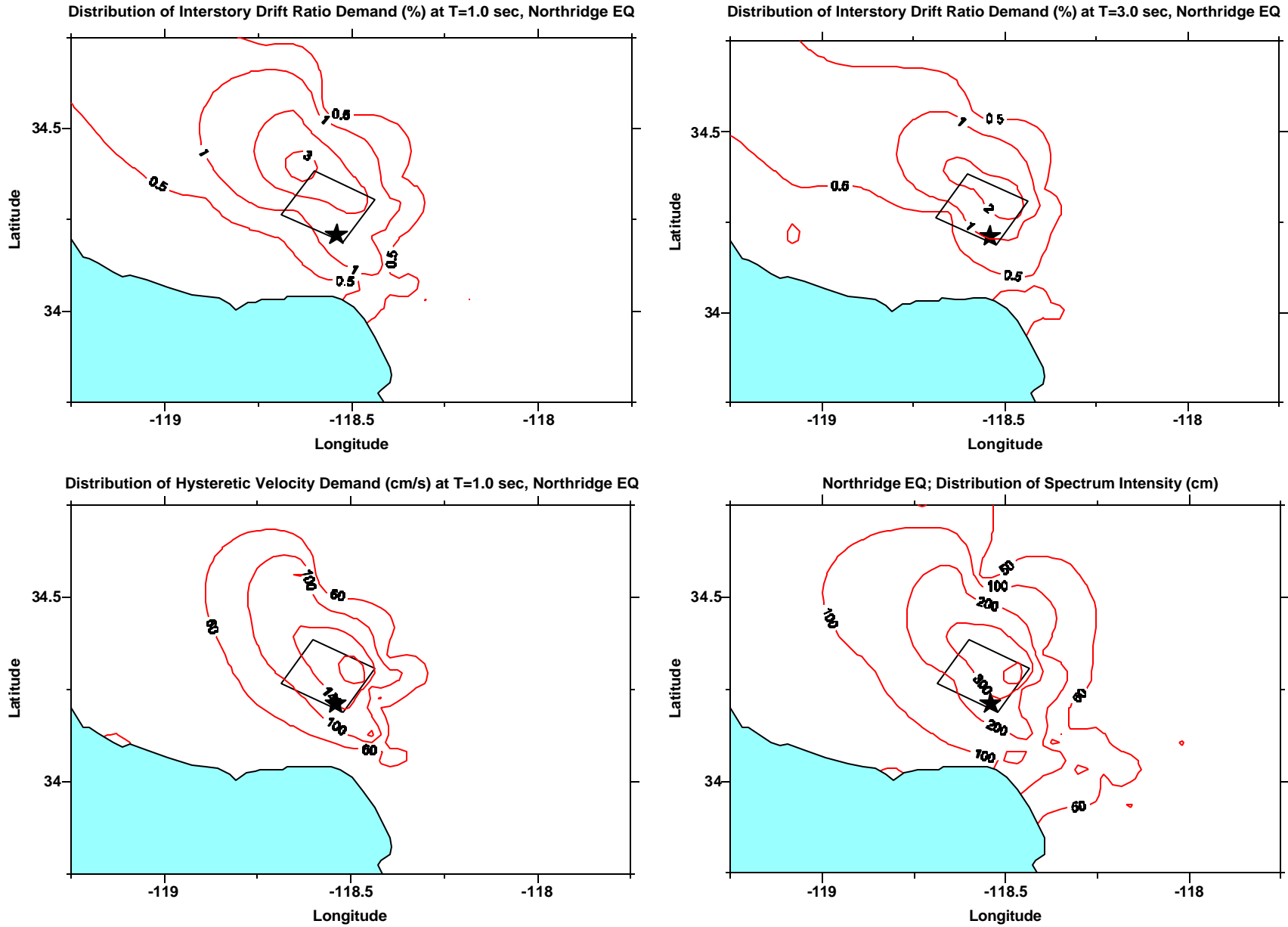


Figure 7: Distribution of interstory drift ratio demand (T= 1, 3 sec); hysteretic velocity demand (T=1 sec) and spectrum intensity, Northridge earthquake.

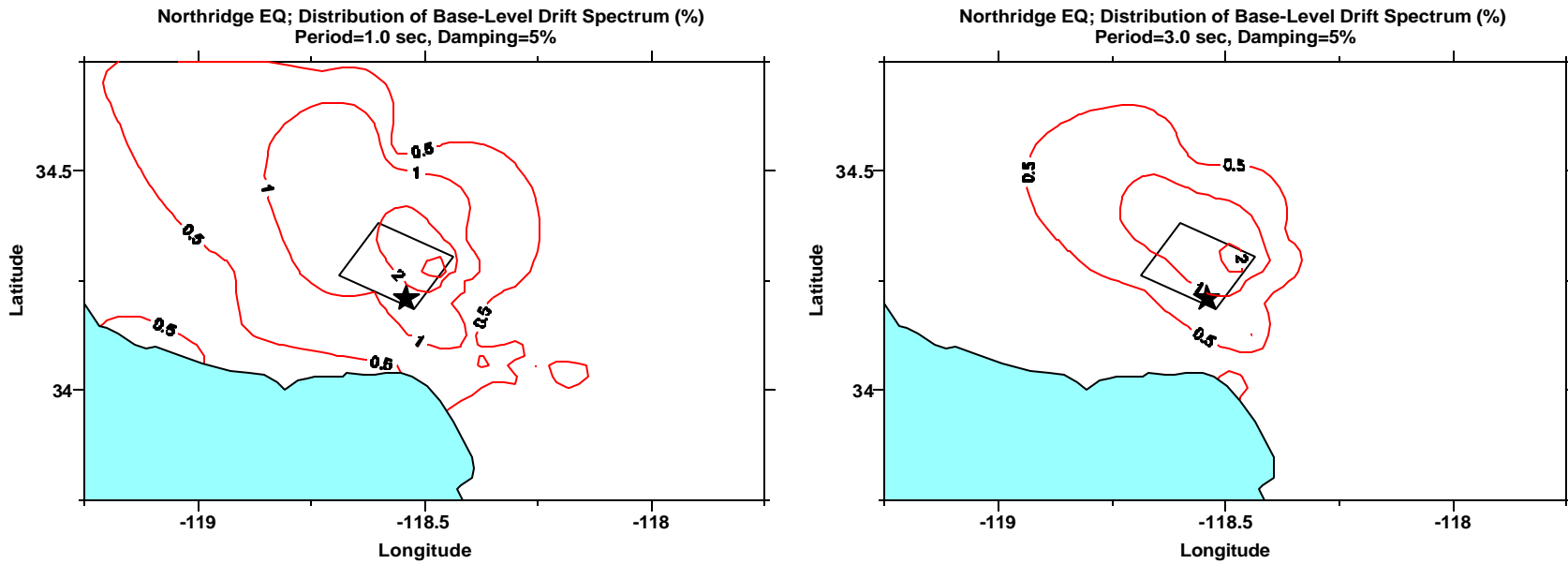


Figure 8: Distribution of drift spectral ordinates at base-level, Northridge earthquake, T=1, and 3 sec.

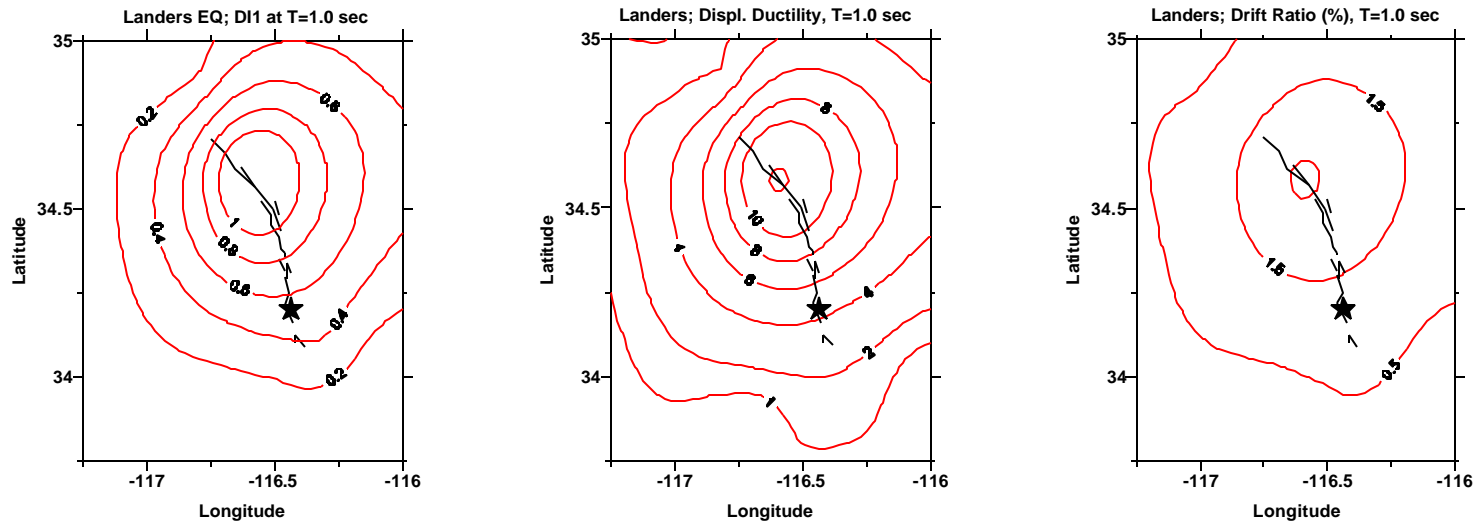


Figure 9: Distribution of damage spectral ordinates, displ. ductility and interstory drift ratio demands, Landers earthquake, T=1 sec.